Rare Metal Materials and Engineering
Volume 45, Issue 6, June 2016
Online English edition of the Chinese language journal

Available online at www.sciencedirect.com
ScienceDirect

Cite this article as: Rare Metal Materials and Engineering, 2016, 45(6): 1386-1390.

ARTICLE

A Comparative Study of Spray-dried and Mechanically-mixed ZrB_2-$MoSi_2$ Composite Coatings Fabricated by Low Pressure Plasma Spray

Mao Jinyuan[1, 2], Liu Min[2], Deng Chunming[2], Mao Jie[2], Zeng Dechang[1]

[1] South China University of Technology, Guangzhou 510640, China; [2] Guangzhou Research Institute of Non-ferrous Metals, Guangzhou 510650, China

Abstract: The agglomerated ZrB_2-$MoSi_2$ composite powder was prepared by spray drying and sintering. The spray-dried ZrB_2-30wt%$MoSi_2$ (SZM) composite coating was manufactured by low pressure plasma spray (LPPS) using the agglomerated powder. For comparison, the mechanically-mixed ZrB_2-30wt%$MoSi_2$ (MZM) composite coating was also prepared by LPPS. The composite powders and the coatings were characterized by X-ray diffraction and scanning electron microscopy. The flowability and the loose density of the agglomerated powders were measured by Hall flow meter and loose density instrument, respectively. Microhardness, porosity and oxidation behavior of the coatings were also investigated. The results show that when the spray-dried powder is sintered at 1200 ℃ for 1 h, its flowability and loose density are up to 25.8 s/50 g and 1.12 g/cm^3, respectively. The distribution of $MoSi_2$ phase in SZM coating is much more uniform than that in MZM coating. Additionally, the SZM coating exhibits a high compactness and much better oxidation-resistance at 1500 ℃ compared to the MZM coating.

Key words: ZrB_2-$MoSi_2$; low pressure plasma spray; oxidation; C/C composites

Carbon/carbon (C/C) composites exhibit excellent high-temperature mechanical properties such as low density, low coefficient of thermal expansion (CTE), high specific strength and good thermal shock resistance[1], so they are considered as promising candidate materials for applications in aeronautics and astronautics fields [2]. However, the oxidation of these composites at temperatures above 723 K in oxidizing atmosphere restricts their applications as high-temperature materials[3].

Several approaches are considered to prevent C/C composites from oxidation at high temperature. Among them, coating is a logical method to solve the problems[4,5]. $MoSi_2$ has proved to be an excellent anti-oxidation material because of the self-sealing performance at high temperature and the high melting temperature of 2030 ℃, which dictates a potential upper use temperature of about 1600 ℃[6]. ZrB_2, a representative of ultra-high-temperature ceramics (UHTCS), has excellent oxidation-resistant property due to B_2O_3 glaze which is one kind of oxides formed by ZrB_2 and oxygen at 1273 K[7]. Moreover, ZrO_2 from the oxidation of ZrB_2 is typical thermal barrier materials[8].

The spray-drying technique is an ideal method for spherical powders preparation. It can significantly improve the flowability of powders and avoid the separation of different powders in a jet or torch. Low pressure plasma spray (LPPS) is a versatile technology which has the advantage to allow for a controlled composition of the operating atmosphere in the chamber, to inhibit oxidation or contamination of the powders and sprayed coatings[9,10].

Although the LPPS technique is widely used in the preparation of coating, few research has been done so far on low pressure plasma sprayed ZrB_2-$MoSi_2$ composite coatings. Moreover, no study was focused on the comparison of oxidation resistance between SZM and MZM coatings.

Received date: June 14, 2015
Corresponding author: Mao Jinyuan, Candidate for Master, South China University of Technology, Guangzhou 510640, P. R. China, Tel: 0086-20-37238263, E-mail: maojy0115@163.com

In the present work, spray-dried and mechanically-mixed powders were prepared. Two kinds of coatings were manufactured using the similar parameters by LPPS. The oxidation resistant behavior of SZM and MZM coatings were investigated. Phase composition and morphology of coatings were characterized and some other features, including porosity and microhardness of coatings were also studied.

1 Experiment

Commercially available ZrB_2 powder with particle size in range of 1~10 μm and $MoSi_2$ powders with a particle size ranging from 1 to 20 μm were chosen as feedstock for SZM and MZM powders. The mixture of ZrB_2-$MoSi_2$ powders with composition of 70 wt% ZrB_2 and 30 wt% $MoSi_2$ as ball-milled for 24 h in deionized water using zirconia milling media to ensure thoroughly mixing of the two components. The slurry of the powder mixture was spray-dried to a composite powder by centrifugal spray dryer (PGZ-10KL, ACMC, China). The parameters of spray drying powder are shown in Table 1.

The spray-dried powder (Fig.1a) was placed in an alumina crucible and sintered at 1200 ℃ in an argon atmosphere box furnace (KBF13Q, Nanjing University Instrument Factory, China). The parameters of sintering (especially temperature) were determined by DSC-TG analysis (STA 449 C, NETZSCH, Germany). The particle size of SZM powder was tested by a laser particle size distribution analyzer (LA-950, HORIBA, Japan). The loose density and flowability of the powder also were measured. The MZM composite powder, consisting of 70 wt% ZrB_2 and 30 wt% $MoSi_2$, was just mechanically mixed for 3 h. The morphology is shown in Fig.1b.

The coatings deposition was carried out by a low pressure plasma spray equipment (AMT-F4 type gun). Argon and hydrogen were used as the plasma forming gases. The deposition parameters of coatings are summarized in Table 2. The powders were preheated at 70 ℃ for 60 min. Graphite was used as substrate. It was roughened using sandpaper and then cleaned with ethanol by ultrasonication. For comparison, MZM coatings were also prepared using the same parameters. Free-standing specimens with a thickness ranging from 100 to 300 um were deposited on the graphite substrates and peeled off for property characterization.

The phase compositions of the powders and coatings were analyzed by X-ray diffraction (X'Pert Pro MRD, PANalytical, Holland). The cross-section morphologies of coatings were observed by field-emission scanning electron microscopy (FE-SEM, NOVA NanoSEM 430, FEI, USA). The composition and element distribution of the coatings were characterized by energy-dispersive spectroscopy (EDS) attached to SEM equipment. Some other characteristics, including microhardness and void content of coatings were also investigated. For evaluating anti-oxidation properties of the coatings, the freestanding coatings were placed in a zirconia crucible in a box type furnace and oxidized at 1500 ℃ in ambient air for 1 h followed by furnace-cooling to room temperature. The mass change of each sample was measured with an electronic balance (sensitivity: 10^{-4} g). The ratios of mass changes to surface areas of the samples were then calculated.

Table 1 Parameters in spray drying

Rotating speed of nozzle/ $r\ min^{-1}$	Inlet temperature/ ℃	Outlet temperature/ ℃
19500	200	120

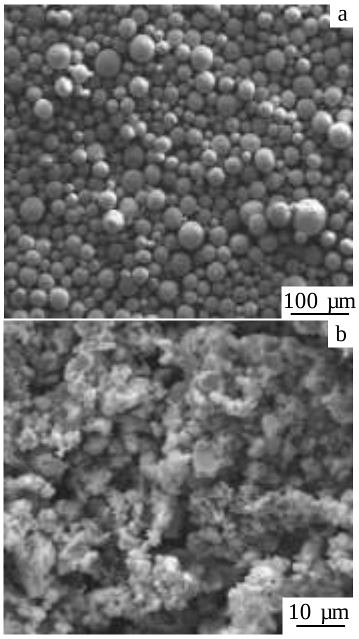

Fig.1 Morphologies of SZM (a) and MZM (b) powders

2 Results and Discussion

2.1 Microstructure of spray-dried powder

Fig.2 shows the SEM morphologies of spray-dried powder. It can be seen from Fig.2a that the spray-dried powder is spherical. And the average particle size is 35.2 um. At higher magnification (Fig.2b), the spherical agglomerated powder consisting of irregular and small ZrB_2 and $MoSi_2$ particles is just bonded by the addition of binder. So the spray-dried powder has low bonding strength and a lot of pores (Fig.2c).

The spray-dried powder without heat treatment is easy to be broken into small pieces when it feeds into high temperature plasma spray jet. When the powder is used for the preparation of coatings, the coatings will show poor quality and the deposition efficiency of the powder will be low.

2.2 Effect of heat treatment on microstructure of the spray-dried powder

Table 2 LPPS parameters for SZM and MZM coatings

Power/kW	Gas Ar/L·min^{-1}	Gas H_2/L·min^{-1}	Spray distance/mm	Carrier gas Ar/L·min^{-1}	Pressure/kPa
50	40	10	170	1.5	40

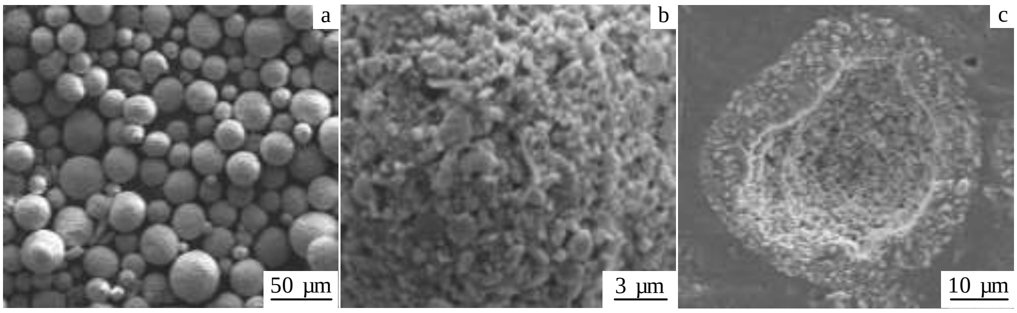

Fig.2 Morphologies of spray-dried ZrB_2-$MoSi_2$ composite powders: (a) low magnification, (b) single powder, and (c) section morphology of single particle

DSC-TG analysis of the spray-dried composite coatings is shown in Fig.3. It can be seen from the TG curve that the mass of the spray-dried powder decreases rapidly with increasing of the temperature from 80 ℃ to 200 ℃, which is related to the evaporation of the residual water. And the obvious decline from 400 ℃ to 500 ℃ indicates the decomposition of binder. Corresponding to the mass loss, there are two evident endothermic peaks at 80 and 389.2 ℃ in DSC curve. The binder is not volatilized completely until 510 ℃. According to the DSC-TG analysis, the processing parameters of heat treatment of the spray-dried powder are determined and shown in Fig.4.

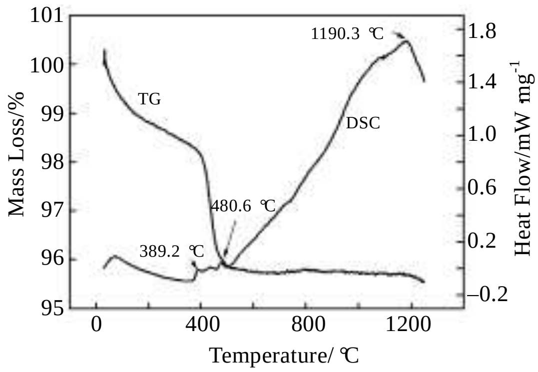

Fig.3 DSC-TG curves of the spray-dried composite powder

Fig.5 shows the SEM images of the spray-dried and heat treated composite powders. It can be seen that the sphericity of the particles is slightly decreased after heat treatment. The residual water and the binder are removed completely. Furthermore, the small primary particles (after ball milling) are sintered and there is no any adhesion between secondary particles (after spray drying). So bonding strength between primary particles increases evidently. At the same time, the flowability and the loose density of the powder are up to 25.8 s/50 g and 1.12 g/cm^3, respectively. And the average particle size is reduced to 27.6 μm (Fig.6). So the spray-dried powder after sintering is more suitable for LPPS.

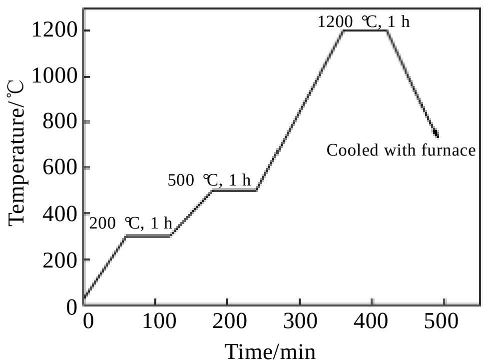

Fig.4 Heat treatment curves of the spray-dried composite powder

2.3 Composition and microstructure of the coatings

Fig.7 shows the XRD patterns of the as-received powders and as-sprayed composites coatings. It can be seen that the phase of $MoSi_2$ can not be detected in the mechanically-mixed ZrB_2-$MoSi_2$ coating, revealing the maldistribution of $MoSi_2$ during the deposition process (Fig.7b). This result is also demonstrated in Fig.8c. For comparison, both ZrB_2 and $MoSi_2$ can be observed in the spray-dried ZrB_2-$MoSi_2$ coating (Fig.7a). Moreover, the tetragonal $MoSi_2$ and hexagonal $MoSi_2$ phases can be detected in the SZM coating. It is believed that the formation of hexagonal $MoSi_2$ is due to the high cooling rate of the deposited molten particles (about 10^6 K/s) [11]. Polished cross-section morphologies and element mappings of the two kinds of ZrB_2-$MoSi_2$ coatings are presented in Fig.8. The structure of the MZM coating exhibits non-compact structure, whereas the SZM coating exhibits a

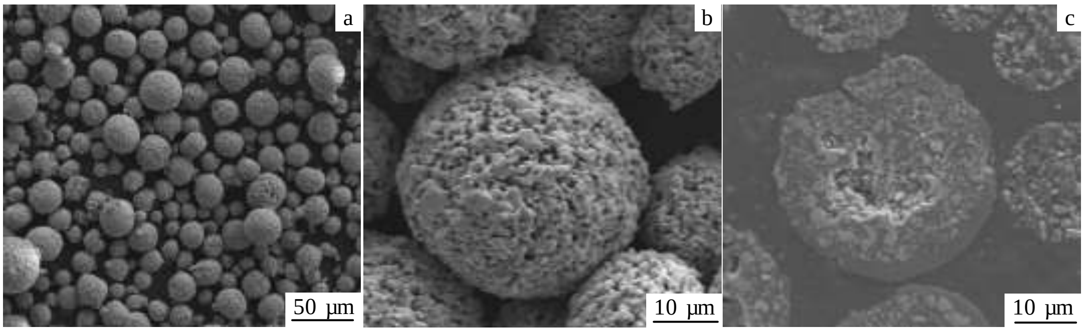

Fig.5 Morphologies of spray-dried ZrB_2-$MoSi_2$ composite powders sintered at 1200 ℃: (a) low magnification, (b) single powder, and (c) section morphology of single particle

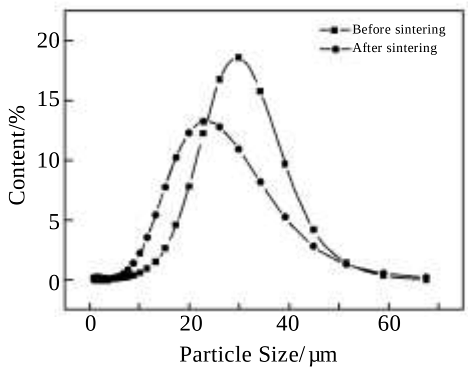

Fig.6 Particle size distribution of spray-dried composite powder

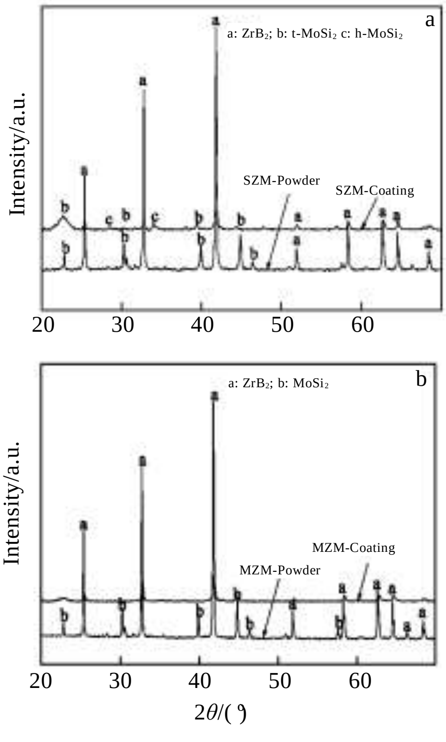

Fig.7 XRD patterns of as-sprayed powders and coatings of SZM (a) and MZM (b)

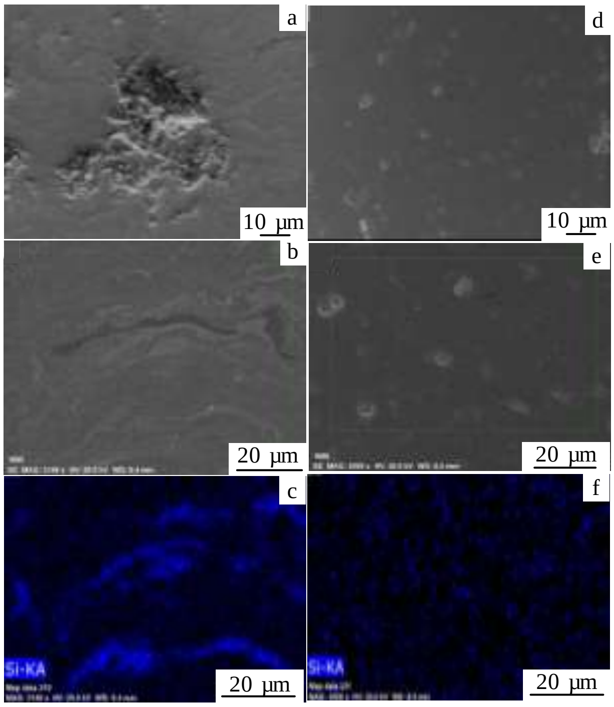

Fig.8 Cross-section morphologies and element mappings of MZM coating (a, b, c) and SZM coating (d, e, f)

dense and homogeneous structure. Void content in MZM coating is (16±2)%, while it is (10±1)% in SZM coating as determined by image analysis. The higher microhardness of SZM coating can be explained by its lower void content. The result of element mapping indicates that the amount of $MoSi_2$ in the MZM coating is limited and its distribution is not uniform (Fig.8c). By contrast, $MoSi_2$ uniformly distributes in the SZM coating (Fig.8f). Both the freestanding SZM and MZM coatings are oxidized at 1500 ℃ to evaluate their anti-oxidation behavior. After oxidized for 1 h, mass gains of SZM and MZM coatings increase by 18.2 and 22.3 mg/cm^2, respectively.

During the oxidation resistance tests at 1500 ℃, the chemical reactions are as follows [8]:

$$2ZrB_2(s) + 5O_2(g) \rightarrow 2ZrO_2(s) + 2B_2O_3(l) \quad (1)$$

$$2MoSi_2(s) + 7O_2(g) \rightarrow 2MoO_3(g) + 4SiO_2(l) \quad (2)$$

B_2O_3 is evaporated at 1500 ℃ due to its low melting –point (445 ℃). Glassy SiO_2 at 1500 ℃ has low oxygen diffusion coefficient which can retard inward diffusion of oxygen. Furthermore it can seal the holes and cracks due to the liquidity on the coating at high temperature. Therefore an excellent oxidation resistance is provided [12].

The amount of SiO_2 depends on the content and the distribution of original silicon-containing phase. For the MZM coating, the distribution of $MoSi_2$ in ZrB_2 matrix is non-uniform, which is confirmed by the results of element mapping (Fig.8c). In addition, the amount of $MoSi_2$ inside the MZM coating is limited. The area lacking $MoSi_2$ is easy to be oxidized. Therefore, the MZM coating is oxidized more seriously in comparison with the SZM coating.

3 Conclusions

1) The spherical agglomerated ZrB_2-$MoSi_2$ composite powder can be prepared by the spray-drying technique. After sintering at 1200 ℃ for 1 h in argon atmosphere, the composite powder is more compact than that before heat treatment and the flowability and loose density of the powder are up to 25.8 s/50 g and 1.12 g/cm^3, respectively. They are suitable for LPPS.

2) The SZM and MZM composite coatings can be manufactured by LPPS. The spray-dried ZrB_2-$MoSi_2$ coating has a dense and homogeneous microstructure compared to the mechanically-mixed ZrB_2-$MoSi_2$ coating. Besides, the SZM coating exhibits lower void content and higher Vickers hardness in comparison with MZM coating.

3) Due to the uniform distribution and controllable quantity of original silicon-containing phase ($MoSi_2$), the oxidation resistant property of SZM coating is better than that of MZM coating at 1500 ℃.

References

1 Zhang Yulei, Li Hejun, Yao Xiyuan *et al*. *Corrosion Science*[J], 2011, 53: 2075

2 Qiang Xinfa, Li Hejun, Zhang Yulei *et al*. *Corrosion Science*[J], 2011, 53: 523

3 Smeacetto F, Salvo M, Ferraris M. *Carbon*[J], 2002, 40: 583

4 Feng Tao, Li Hejun, Yang Xi *et al*. *Corrosion Science*[J], 2013, 72: 144

5 Smeacetto F, Ferraris M, Salvo M. *Carbon*[J], 2003, 41: 2105

6 Park Soo-Jin, Seo Min-Kang. *Carbon*[J], 2001, 39: 1229

7 Feng Tao, Li Hejun, Shi Xiaohong *et al*. *Corrosion Science*[J], 2013, 67: 292

8 Zhang Wuzhuang, Zeng Yi, Lemuel Gbologah *et al*. *Transactions of Nonferrous Metals Society of China*[J], 2011, 21: 1538

9 Zhang Y J, Sun X F, Zhang Y C *et al*. *Materials Science and Engineering A*[J], 2003, 360: 65

10 Zhang X C, Xu B S, Xuan FZ *et al*. *Journal of Alloys and Compounds*[J]. 2009, 473: 145

11 Fei Xiaoai, NiuYaran, Ji Heng *et al*. *Ceramics International*[J], 2011, 37: 813

12 Yoon J K, Lee K H, Kim G H *et al*. *Journal of the Electrochemical Society*[J], 2004, 151B: 309

低压等离子喷涂制备喷雾干燥型与机械混合型 ZrB_2-$MoSi_2$ 复合涂层的比较研究

毛金元 [1,2]，刘 敏 [2]，邓春明 [2]，毛 杰 [2]，曾德长 [1]

(1. 华南理工大学，广东 广州 510640)

(2. 广州有色金属研究院，广东 广州 510650)

摘 要：利用喷雾干燥与真空烧结技术制备团聚型ZrB_2-$MoSi_2$复合粉末，以这些粉末为原料，通过低压等离子喷涂法制备了ZrB_2-30%$MoSi_2$ (质量分数)复合涂层(SZM涂层)。作为对比，利用机械混合粉末制备了ZrB_2-30%$MoSi_2$复合涂层(MZM涂层)。借助SEM、XRD和EDS等对涂层的组织结构进行研究，并利用霍尔流速计和松装密度计对团聚粉末的流动性和松装密度进行了测试。此外，对涂层的显微硬度、孔隙率和氧化特性均进行了研究。结果表明：喷雾干燥粉末在1200 ℃真空烧结1 h后，它的流动性和松装密度分别达到 25.8 s/50 g 和 1.12 g/cm^3。与MZM涂层相比，SZM涂层中的$MoSi_2$分布更加均匀，而且结构更加致密。所以团聚粉末制备的涂层在1500 ℃表现出更好的抗氧化性能。

关键词：ZrB_2-$MoSi_2$；低压等离子喷涂；氧化；碳/碳复合材料

作者简介：毛金元，男，1990 年生，硕士生，华南理工大学，广东 广州 510640，电话：020-37238263，E-mail: maojy0115@163.com